THE EFFECTS OF ACCESSORY PROTEINS ON ENaC FUNCTION

by

Esther Lee, B.A.

A thesis submitted to the Graduate Council of
Texas State University in partial fulfillment
of the requirements for the degree of
Master of Science
with a Major in Biochemistry
December 2014

Committee Members:

Rachell Booth, Chair

Wendi David

Kevin Lewis

COPYRIGHT

by

Esther Lee

2014

FAIR USE AND AUTHOR'S PERMISSION STATEMENT

Fair Use

Duplication Permission

DEDICATION

This is dedicated to Adam. Without him, none of this would have ever been possible.

ACKNOWLEDGEMENTS

First, I must thank Dr. Rachell Booth for everything she has done for me. She took a chance on a music major who had no experience or knowledge. Her patience, guidance, and never-ending encouragement are what carried me through this program. She has changed my life, and words will never be able to express how grateful I am to her.

I would like to thank the members of the Booth lab for all of their help and encouragement. I would not have survived the first few months in lab without the help of Samantha Swann, and these last few months without Jose Reyes.

I need to thank Amber Lucas and Daniel Horn for being such amazing friends and labmates. I will always remember and cherish all of the laughter and late nights we have shared during this program. One day, I hope to be as brilliant as the two of them.

I also want to thank Abraham Amos for being the most extraordinary study partner, motivator, and friend imaginable. Our friendship has pushed me to be a better student, scientist, but most importantly, a better person. I would not have made it this far without his constant encouragement and faith.

Finally, I would like to thank my family and friends for always being my one true constant through this entire journey. All of their kind words and emotional support have gotten me to the end. I owe a special thanks to Terry Martinez who graciously edited this document on numerous occasions. I especially want to thank my husband, Adam. Without his support, sacrifice, and endless patience, I would not be where I am today.

TABLE OF CONTENTS

Page

LIST OF TABLES

Table **Page**

LIST OF FIGURES

ABSTRACT

Maintaining homeostasis is crucial for perpetuating good health. Any imbalance, such as hypertension, can lead to heart and kidney disease. Epithelial sodium channels, also known as ENaC, constitute the rate-limiting step of sodium reabsorption in the distal tubules of the nephron in the kidneys. It is here the final, yet critical, 3% to 5% of sodium reabsorption that dictates blood pressure occurs. In this study, β-ENaC was cloned into pESC-Leu and pESC-Leu/γ in order to further characterize accessory proteins in yeast screens using the heterotrimeric channel. An antibody screen against the subunits of ENaC was then performed using murine principle kidney cortical collecting duct (mpkCCD) cells as a means of identifying a primary antibody for western blotting. RNA Interference studies in mpkCCD cells were also performed. Knockdown of the accessory proteins TMED2 and TMP21 through RNAi indicated a decrease in ENaC expression. These results indicated that TMED2 and TMP21 are essential for ENaC trafficking.

CHAPTER I

Introduction and Literature Review

Ion regulation in Mammalia plays a vital role in maintaining homeostasis. The balance of water and solute concentration within the blood is pivotal to maintaining ideal physiological stability for optimal health and longevity. Imbalances in ion levels, particularly sodium, can result in hypertension, eventually leading to kidney failure, heart disease, stroke, and death[1]. According to the Centers for Disease Control and Prevention, the average American over the age of two consumes seven times the adequate amount of sodium required for proper daily function[2]. Among the human population, high blood pressure is the most common but treatable disease[3]. With 67 million American adults and over 1 billion individuals worldwide suffering from hypertension, understanding the mechanism by which sodium is regulated in the body is crucial[3,4].

As sodium is consumed, it is absorbed by cells in the body before entering into the bloodstream. Sodium enters into cells through membrane ion channels, which are integral proteins embedded within the cell membrane. These transmembrane channels are responsible for regulating the

ion flow in and out cells in accordance with the cell gradient. Though there is a vast diversity in structure among ion channels, the majority of these proteins are composed of multiple subunits[5]. The proper composition, folding, and oligomerization of ion channels subunits are critical for function[5]. Alterations, such as mutations, to the channel can lead to imbalances in homeostasis and disease.

Among the diverse membrane ion channels are amiloride-sensitive, voltage-independent sodium channels known as epithelial sodium channels (ENaC). They are responsible for the passive transport of sodium across tight epithelia. Though epithelial sodium channels are highly selective for Na^+ ions, they also allow for the movement of Li^+ ions into the cell[6]. ENaCs are expressed on the apical membranes of polarized epithelial cells in a multitude of tissues such as the airway, alveoli, sweat glands, GI tract, and the urinary tract[7].

Electrolytic balance in the blood is dependent upon ENaC found in the kidneys, more specifically, in the cortical collecting ducts of the nephron (FIG 1). The nephron is the functional unit of the kidneys, with each kidney comprised of about a million nephrons[3]. Filtration of the blood, as well as the necessary sodium reabsorption,

begins when unfiltered blood enters into the glomerulus within the nephrons. The filtered blood is returned to circulation through the renal vein, while the filtrate (urine) travels into the proximal tubules, where 60% of the necessary nutrients and ions will be reabsorbed back into the body. The next 30% of the filtrate will be reabsorbed while moving through Henle's loop where water is simultaneously filtered out, concentrating the ions. The last of the filtrate enters into the cortical collecting duct of the distal tubules where the final 3% to 5% of sodium reabsorption occurs through ENaC before it is excreted from the body[3]. Though this final percentage may seem numerically small, it is here that the critical fine-tuning of electrolytic balance, and ultimately blood pressure, is determined[8].

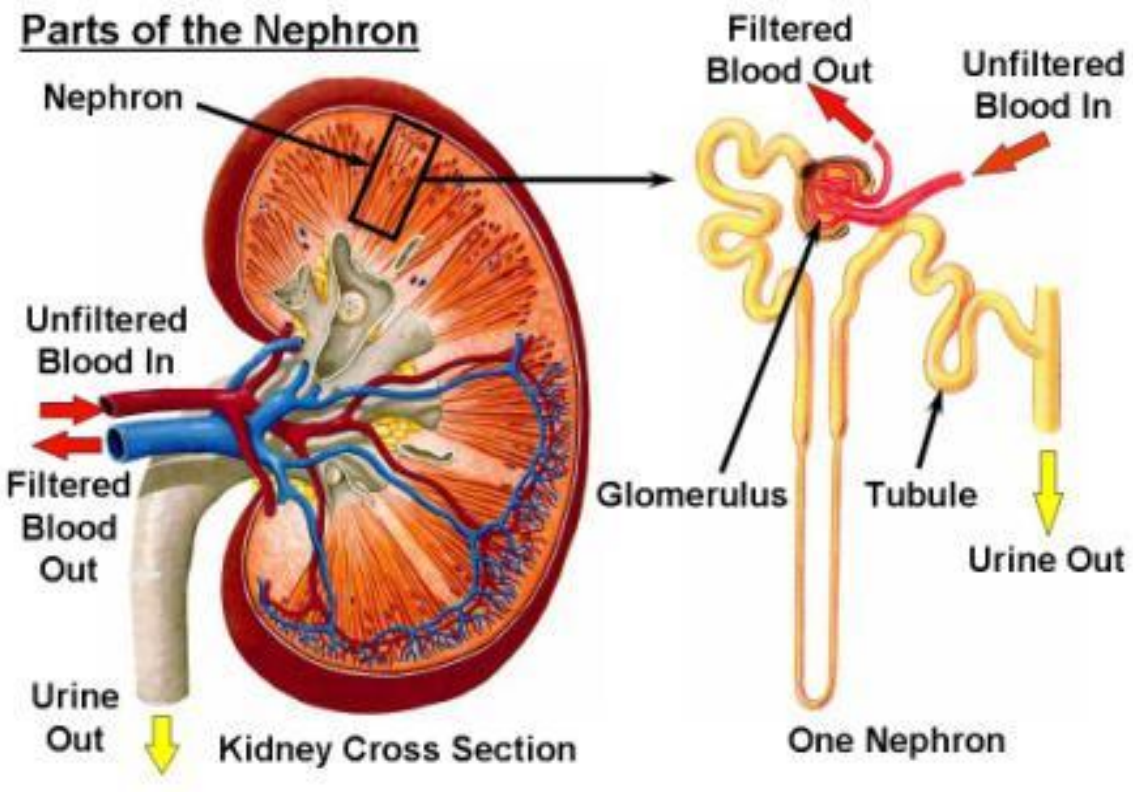

FIG 1. Diagram of the nephron. Unfiltered blood enters into the nephron from the circulatory system to be filtered and excreted. Before excretion, nutrients and ions required for homeostasis are reabsorbed back into the blood. Image from Guyton, A.C. and Hall, J.E. (2006) *Textbook of Medical Physiology*. Philadelphia: Elsevier Saunders. pp. 310.

The reabsorption of sodium from urine to blood through epithelial cells occurs in two steps. First, sodium travels through the pore of ENaC (apical membrane), moving down its electrochemical gradient into the cell (FIG 2). This is the rate-limiting step in sodium absorption[9] and creates an electrochemical driving force for potassium ions to be secreted out into the lumen (urine)[10]. Once in the cell,

sodium is expelled into the blood through a Na^+/K^+ ATPase channel located on the basolateral membrane of the epithelial cell[8]. Each conformational change of the channel releases three sodium ions into the blood while transporting two potassium ions into the cell. This mechanism is driven by the hydrolysis of ATP, and controls the ion levels within the cells and volume of fluid on either side of the basolateral membrane[8].

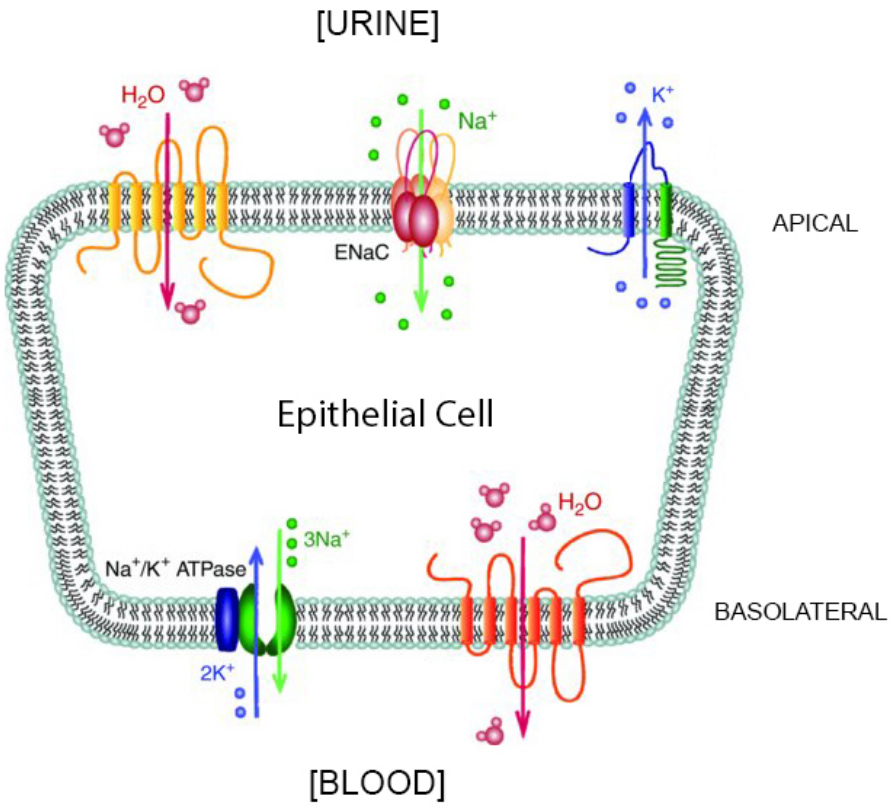

FIG 2. Schematic of sodium absorption. Sodium and water from the urine enters through ENaC into the epithelial cell, where it is then pumped into the blood through a Na^+,K^+-ATPase. Image from Staruschenko, A. (2012) *Comprehensive Physiol.* 2, 1541-1584.

ENaC is a member of the ENaC/Degenerin superfamily of cation channels. Members of this superfamily are classified by their structural homology that has been highly conserved through organisms (FIG 3). Channels in the ENaC/Degenerin family all have a large extracellular loop that is connected by two transmembrane alpha helices, with short amino and carboxylic acid end termini within the cytoplasm[8].

Notable members of the ENaC/Degenerin superfamily include the acid-sensing ion channels (ASIC), which are found in the nervous system. They are sodium channels that are modulated through extracellular protons. The ripped pocket/pickpocket channels (RPK/PPK) are found in *Drosophila* ovary and testes, and activated through transduction of mechanical stimuli from heat. The degenerin channels (DEG) in *Caenorhabditis elegans* facilitate sodium absorption through mechanosensory behavior[10].

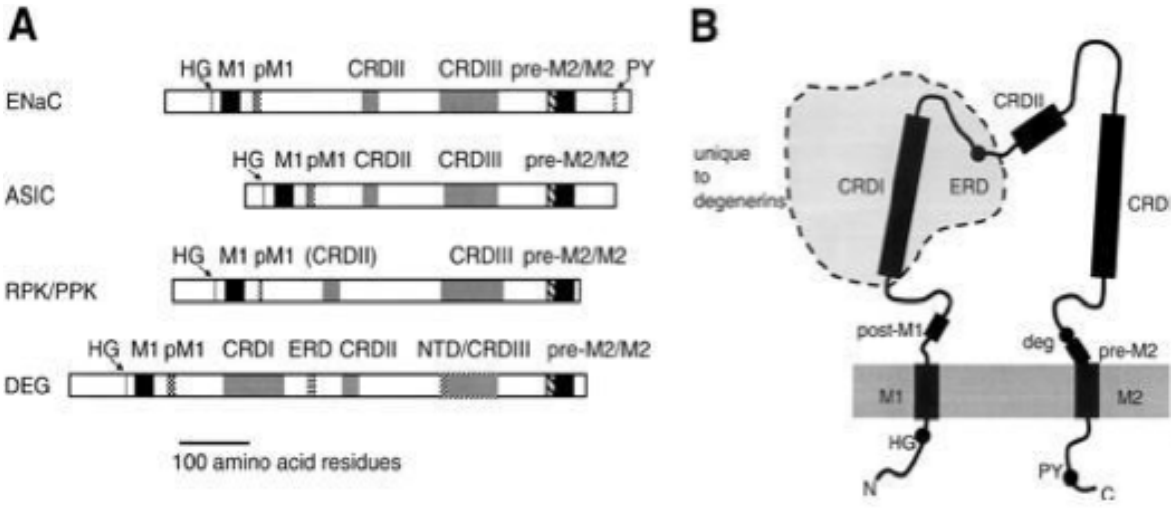

FIG 3. Genetic conservation in ENaC/DEG family. (A) Linear comparison of homologous regions within the primary sequence of different members of the superfamily. **(B)** Topology of an individual subunit. Image from Kellenberger, S. and Schild, L. (2002) *Physiol. Rev.* 82, 735-767.

Unlike channels for potassium, chloride, and water, which appeared during the early stages of evolution, the ENaC/Degenerin genes are only present in animals with organs that have evolved to specialize in reproduction, digestion, and coordination. All members of this superfamily transport sodium, yet demonstrate a wide array of functions and tissue distribution, making the heterogeneity unique among other ion channel families[10].

Structurally, ENaC is a heteromultimer protein whose channels are comprised of several homologous subunits. There are currently four subunits that have been identified: α, β, γ, and δ. The δ-ENaC subunit is believed to be limited to the brain and reproductive tissues, and

functions primarily as a substitute for the α-ENaC subunit[8].

In the kidneys, fully functional ENaC is composed of α-, β-, and γ-ENaC subunits, where they share between 30%-40% homology[11] (FIG 4). When expressed as an α, β, and γ heterotrimeric protein, studies have indicated there is more than a 100-fold potentiation over ENaC that is α homomeric or a lesser heteromeric coexpressing only two subunits[8,12]. Regardless of composition, the α-ENaC subunit must be expressed for ENaC to be functional[13].

Currently, the exact structure of ENaC has yet to be elucidated. It has previously been suggested that the channel is comprised of a 2α:1β:1:γ or 3α:3β:3:γ stoichiometry. More recent studies, including the crystallization of the acid-sensing ion channel 1 (ASIC1), support the probability of ENaC being a trimer[14]. Using atomic force microscopy, Stewart *et al.* revealed the earlier misconceptions of a four or nine subunit stoichiometry was likely due to the subunits of ENaC each producing a higher order structure containing two to three individual trimers[11].

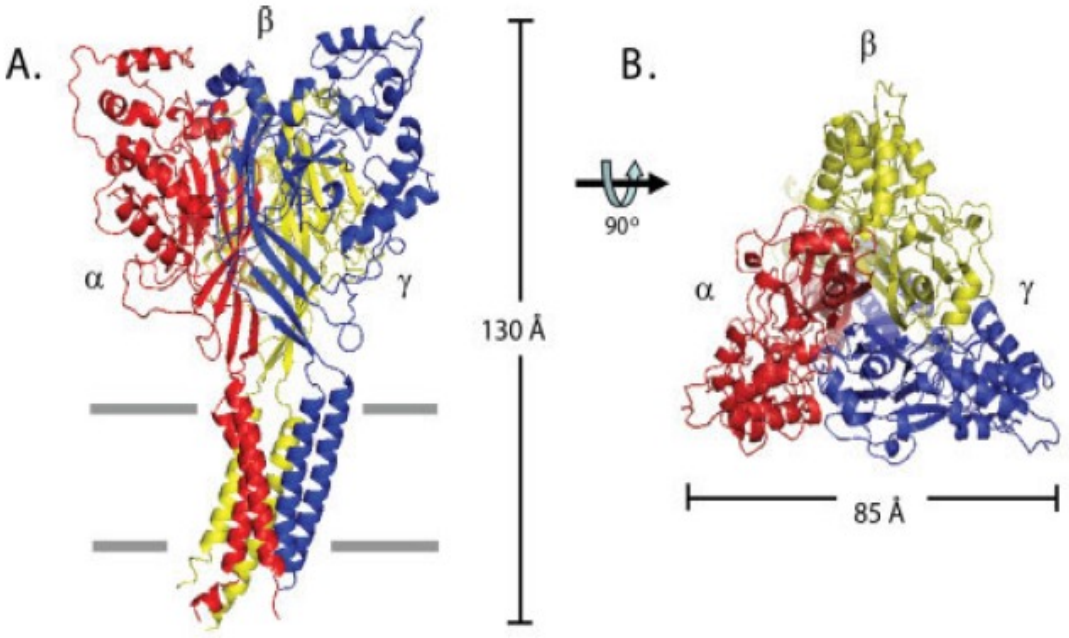

FIG 4. Predicted structure of ENaC. (A) Ribbon structure prediction of ENaC based on the ASIC1 crystal structure. Each subunit contributes to the pore, forming a heterotrimer. **(B)** View of the ribbon structure from the top, looking down the pore formed by the subunits. Image from Stockand, *et al*. (2008) *IUBMB Life* 60, 620-628.

ENaC is constitutively active while imbedded within the luminal membrane of cortical collecting duct epithelia. The amount of sodium absorption is dictated by the quantity of the ENaC present in the cell membrane. Regulation of ENaC expression is under the control of both hormones and other proteins. During homeostatic conditions, ENaC is mostly found in vesicular pools within the intracellular space of the cell[9].

Increases of ENaC cell surface expression occurs in two phases: the early phase, over one to three hours, and

the late phase, which begins around hour six and can last for several days[9]. In times of low blood pressure, the renin-angiotensin-aldosterone cascade is activated, leading to an increase in ENaC activity in the cell surface and Na^+/K^+-ATPase stimulation in the basolateral membrane[10,13]. Renin is released from the kidneys, which converts angiotensinogen to angiotensin I. Angiotensin I is then converted to angiotensin II, stimulating the release of the hormone aldosterone[8]. As a result, aldosterone is the most potent stimulator of α-ENaC expression in the distal tubules.

Once in the cell, aldosterone binds to the mineralocorticoid receptor in the cytosol. The hormone-receptor complex is then translocated to the nucleus where it represses the transcription of aldosterone-repressed transcripts (ARTs) and induces transcription of α-ENaC mRNAs and aldosterone-induces transcripts (AITs)[10]. Therefore, ARTs and AITs have pivotal roles in aldosterone induced transepithelial sodium absorption by upregulating ENaC and Na^+/K^+-ATPase.

The early phase of aldosterone-induced sodium absorption does not seem to occur from an increase in ENaC transcription, but rather from the induction of accessory protein transcripts that aid in ENaC trafficking and

function. One such protein is serum- and glucocorticoid inducible kinase 1 (SGK1)[9]. The mechanism as to how SGK directly stimulates the upregulation of ENaC is still unclear. Indirectly, the PY motif of SGK1 phosphorylates the WW domains within the accessory protein Nedd4-2, which provides a docking site for the protein 14-3-3[8]. This is shown to prevent Nedd4-2 from interacting and removing ENaC from the cell surface, thus increasing sodium absorption[9,15] (FIG 5).

During the late phase, cell surface expression is attributed to an increase in α-ENaC transcription and thus an increase in the functional α-ENaC subunit. Transcription of the β- and γ-ENaC subunits is believed to be continuous. It has been hypothesized that α-ENaC transcription is the rate-limiting step in functional channel formation; therefore, transcriptional increase of the α-ENaC subunit would increase the delivery of functional ENaC to the surface of the cell[9].

Synergistically, with aldosterone, the hormone vasopressin also activates the level of cell surface ENaC[16]. In response to changes in blood volume and osmotic pressure, vasopressin is released by the hypothalamus and binds to V2 receptors on the basolateral membrane of the cell[16]. This binding event activates adenylate cyclase,

which increases the level of cellular cAMP[9]. As a result, ENaC subunits stored in vesicle pools are mobilized by cAMP to the apical surface[17].

In times of hypertension, NEDD4-2, a member of the ubiquitin ligase family, mediates ENaC endocytosis. The WW domains of NEDD4-2 interact with the PY motifs in the C-terminus of ENaC subunits[9]. This protein-protein interaction allows for the transfer of ubiquitin from NEDD4-2 to ENaC, which eventually leads to polyubiquitination of ENaC, thus tagging it for cell surface removal[18]. Once removed, ENaC is either held for reimplementation into the cell membrane or sent for degradation[18]. As ENaC is removed from the membrane, the number of sodium entering into the cell is quickly decreased.

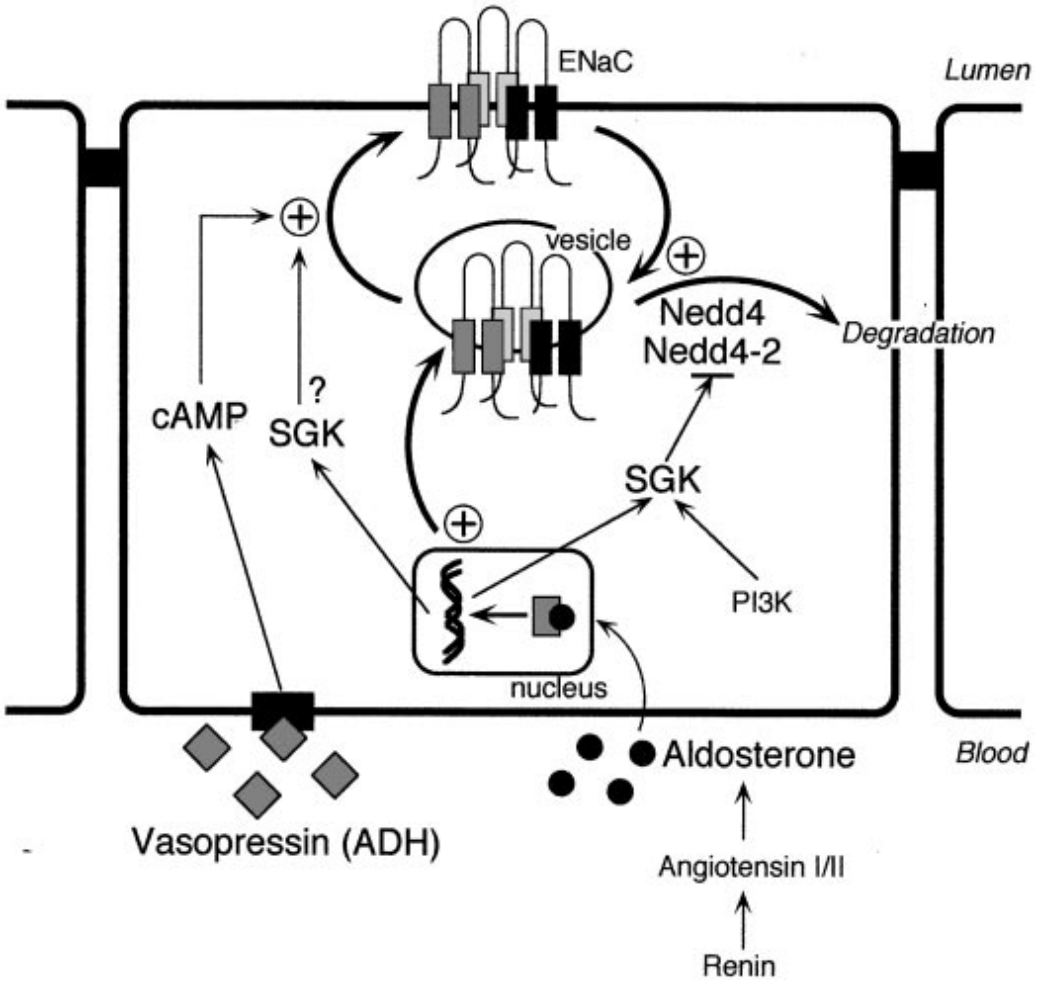

FIG 5. ENaC regulation. Expression of ENaC is increased by the hormones aldosterone and vasopressin. Nedd4-2 aids in ubiquitination, which leads to the endocytosis of ENaC for downregulation. Image from Snyder, P. (2002) *Endocr. Rev.* 23, 258–275.

Recent studies have indicated that ENaC regulation is also under the control of circadian oscillations[16]. Studies done by Gumz and associates found that silencing of the circadian clock protein Period 1 significantly decreases α-ENaC mRNA expression[19]. The results suggest an important

role of the circadian clock in sodium regulation.

A pharmacological regulator of ENaC is amiloride and its analogs. It has been well demonstrated that ENaC, as well as the rest of the superfamily, possesses a high affinity for amilorde, a potassium-sparing diuretic. It works by competing with sodium and directly blocking the pore of the channels[20]. Though the exact mechanism of interaction between amiloride and ENaC is still unclear, it has been hypothesized that the guanidium portion of amiloride interacts with the ENaC's selectivity filter while the pyrazine moiety binds to the area preceding the M2 region of ENaC[20]. As a result, amiloride hinders sodium's entrance into the cell.

Any changes in the structure of ENaC can lead to functional failure and often times, disease. Mutations in ENaC are responsible for two rare genetic diseases: pseudohypoaldosteronism type 1 (PHA-1) and Liddle's Syndrome.

PHA-1 is a rare genetic disease characterized by severe salt wasting/hypotension, dehydration, hypernatremia, hyperkalemia, and metabolic acidosis. It is caused by deletion or frameshift mutations in N-terminus of the α-, β-, or γ-ENaC subunit or by mutations in the mineralocorticoid receptor[3].

Liddle's Syndrome is a severe form of hypertension and salt sensitivity due to overactive ENaC. In addition to extreme hypertension, Liddle's Syndrome can also lead to hypokalemia, metabolic alkalosis, and low plasma renin activity[3]. This disease is a result of mutations caused by a deletion of about 75 amino acids from the C-termini of the β- and γ-ENaC subunits[3]. The deletions affect the PY motif that interacts with the WW domain of NEDD4-2. Consequently, cell surface ENaC does not undergo endocytosis, causing a continuous flow of sodium into the cell.

Murine principle kidney cortical collecting duct (mpkCCD) cells are an immortalized clonal cell line from mouse kidneys established by Bens and associates[21]. mpkCCD cells were first harvested from SV-PK/Tag transgenic mice[21]. These cells naturally express fully functioning ENaC at the cell surface and possess the same properties and sensitivities as those found in the kidney[21]. Once cultured, the cells form polarized monolayers, allowing for a multitude of sodium transport studies.

Previous studies in the Booth lab, using a yeast deletion library, have identified possible accessory proteins that might affect ENaC function. Each strain with a different, individual gene knocked out was transformed with a plasmid that can overexpress α-ENaC in order to

assess salt sensitivity in yeast cells. Survival dilution growth assays were carried out on the transformed deletion strains to see how the deleted genes affected cellular response to high levels of ENaC function in high salt growth media.

From these studies, the accessory proteins transmembrane emp24 domain trafficking protein 2 (TMED2) and transmembrane emp24-like trafficking protein 10 (TMP21) were identified from yeast strains YGL054C and YML012W. Missing the TMED2 and TMP21 gene, respectively, that were transfected with α-ENaC did not seem to exhibit as much growth inhibition compared to that of the wildtype with α-ENaC (FIG 6). This indicated that these genes were somehow important to the function of ENaC and further analysis in mammalian cells was conducted.

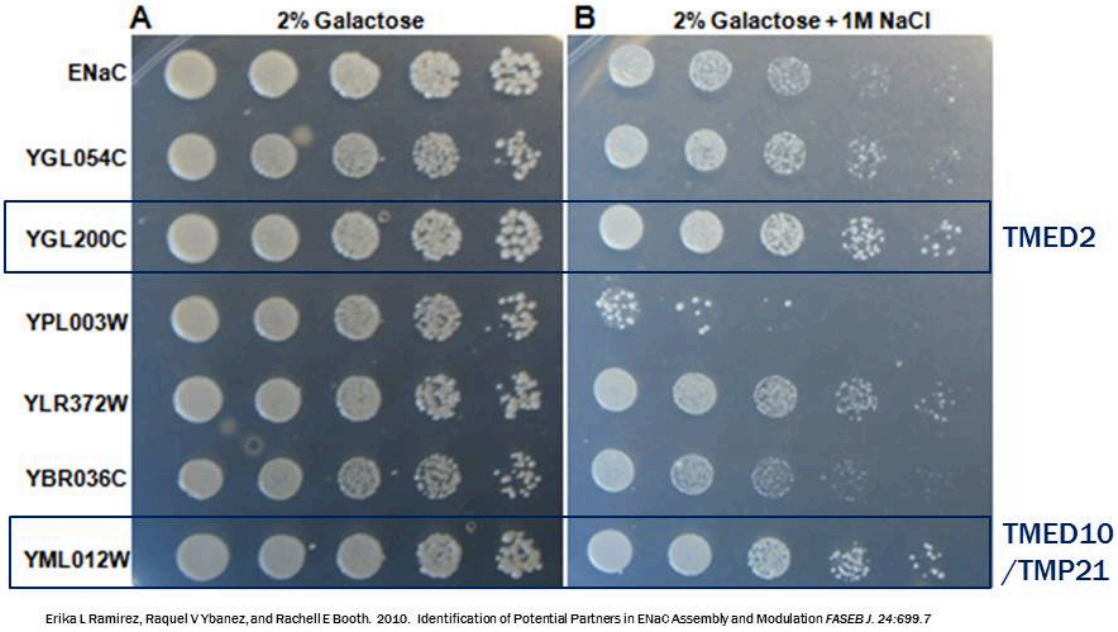

FIG 6. Survival dilution growth assay of knockout yeast. (A) Yeast strains transformed with α-ENaC on 2% galactose plates with minimal NaCl. (B) Yeast strains transformed with α-ENaC on 2% galactose plates with 1 M NaCl. Yeast with the YGL200C (TMED2) and YML012W (TMP21) genes deleted displayed much more growth inhibition in the presence of increased NaCl.

TMED2 and TMP21 are members of the TMED/p24 protein family of trafficking proteins. Members of this family are involved in many processes including chaperoning, vesicle formation, cargo selection, transport to the Golgi apparatus, and finally transport to the cell membrane[22]. The members of the TMED/p24 family structurally share the same distinct functional domains and fall into four subfamilies[22]. Studies have indicated that knockdown or deletion of one TMED protein can induce the loss of

expression of TMED proteins from other subfamilies[22]. This would disrupt multiple processes within the ER, Golgi, and cell membrane.

This study has used mpkCCD cells as a model in order to identify the effects of accessory proteins on ENaC function. siRNAs were used to silence TMED2 and TMP21, which were speculated to aid in the trafficking of ENaC to the apical membrane. These studies have contributed to the further understanding of ENaC transport as well as provided further insight into the complex roles accessory proteins play in their interaction and relationship with ENaC.

CHAPTER II

Materials and Methods

Sequence Analysis

A sequence analysis was performed using the *Saccharomyces* Genome Database (www.yeastgenome.org). The protein sequence for each yeast strain of interest was found in the database. Mouse homologs for those strains were then identified from the yeast protein sequence using Basic Local Alignment Search Tool (BLASTP) for standard proteins at National Center for Biotechnology Information (www.ncbi.nlm.nih.gov).

CLONING

PCR

The pCMV-Myc/β-ENaC plasmid DNA was donated by the Stockand Lab (UTHSCSA). Custom primers against the plasmid DNA (Table 1) were designed and synthesized by Integrated DNA Technologies (Coralville, IA). PCR was performed using 117.0 ng pCMV-Myc/β-ENaC as template, 500 µM dNTPs (New England BioLabs, Ipswich MA), 1.0 µM each of forward and reverse primers, 1X Thermopol Buffer (New England BioLabs), and 2 units of Vent DNA Polymerase (New England BioLabs) in

a total reaction volume of 50 µL. The reaction was run under the following contitions: 95°C for 2 minutes, 25 cycles of 95°C for 30 seconds, 55°C for 30 seconds, and 72°C for 1 minute, and finished with a single cycle at 72°C for 2 minutes. The PCR product was analyzed via agarose gel and then cleaned using QIAquick Gel Extraction Kit, (Qiagen) according to the manufacturer's protocol for cleaning DNA from enzymatic reactions.

Table 1. PCR primers for pCMV-Myc/β-ENaC.

PRIMER	SEQUENCE
FORWARD	5'-CGAACTCGAGCTTATGCCAGTGAAGA-3'
REVERSE	5'-GCAAGCTAGCCTAGATGGCCTCCACC-3'

RESTRICTION DIGESTION

Restriction digestions for pCMV-Myc/β-ENaC, pESC-Leu yeast expression vectors (Agilent Technologies, Santa Clara, CA), and pESC-Leu/γ-ENaC yeast expression vectors were set up using 2.5 µg DNA, 1X CutSmart Buffer (New England BioLabs), 20 units of XhoI (New England BioLabs), and 10 units of NheI (New England BioLab) in a total volume reaction of 50 µL. All digestions were incubated overnight

at 37°C. The vector digestions were dephosphorylated using 1X Antarctic Phosphatase Reaction Buffer (New England BioLabs) and 5 units of Antarctic Phosphatase (New England BioLabs) according to the manufacturer's protocol. A 1X concentration of EndoR Stop sample buffer (100 mM 0.25 M ethylenediaminetetraacetic acid (EDTA) at pH 8.0, 50% v/v glycerol, 1% w/v SDS, 0.1% w/v bromophenol blue) was added to all digestions.

AGAROSE GEL ELECTROPHORESIS

A 0.8% w/v Tris-acetate-EDTA (TAE) agarose gel was loaded with DNA samples and run in 1X TAE (Thermo Scientific) buffer at 85 volts for 90 minutes. The gel was then stained with ethidium bromide and visualized under ultra-violet light. DNA fragments were excised and cleaned using the QIAEX II Gel Extraction Kit (Qiagen) and its recommended protocol.

LIGATION

A 3:1 molar insert to vector ratio along with 1X T4 DNA Ligase (New England BioLabs) and 400 units of T4 DNA Ligase (New England BioLabs) were used in a 20 µL ligation reaction. The reaction was incubated at room temperature for 30 minutes. Five microliters of the ligation reaction

was transformed into NEB 5-alpha Competent *E.coli* cells (New England BioLabs) using the New England BioLabs High Efficiency protocol. The serial dilution from the protocol was not performed, but rather cells were directly plated after incubation onto lysogeny broth plates with ampicillin. Plates were incubated at 37°C overnight. Plasmids from the cells were isolated using the QIAprep Spin Miniprep Kit (Qiagen) according to the manufacturer's protocol. Water was used for DNA elution.

CELL CULTURE

Complete Media

mpkCCD cells were generously donated by the Stockand Laboratory at the University of Texas Health Science Center at San Antonio. The media, reported in v/v concentration, for mpkCCD cells was as follows: 45.8% Dulbecco's Modified Eagle's Medium (DMEM) (Corning Life Sciences, Tewksbury, MA), 45.8% Ham's F-12 (Corning Life Sciences), 0.005% Dexamethasone (Sigma-Aldrich, St. Louis, MO), 0.915% 100X Insulin/Transferin/Selinate (Sigma-Aldrich), 0.0009% 10^{-4} M Triiodothyronine (EMD Millipore, Darmstadt, Germany), 0.009% Epidermal Growth Factor (EGF) (Sigma-Aldrich), 1.83% HEPES (Sigma-Aldrich), 0.915% 200 mM Glutamine (Corning Life Sciences), 1.83% Fetal Bovine Serum (FBS) (Thermo

Scientific, Rockford, IL), 2.05% 10% D-Glucose (BD, Franklin Lakes, NJ), 0.915% Penicillin/Streptomycin (Corning Life Sciences).

Serum Free Media

Serum free media for siRNA transfections was as follows: 45.8% Dulbecco's Modified Eagle's Medium (DMEM) (Corning Life Sciences, Tewksbury, MA), 45.8% Ham's F-12 (Corning Life Sciences), 0.005% Dexamethasone (Sigma-Aldrich, St. Louis, MO), 0.915% 100X Insulin/Transferin/Selinate (Sigma-Aldrich), 0.0009% 10^{-4} M Triiodothyronine (EMD Millipore, Darmstadt, Germany), 0.009% Epidermal Growth Factor (EGF) (Sigma-Aldrich), 1.83% HEPES (Sigma-Aldrich), 0.915% 200 mM Glutamine (Corning Life Sciences), 2.05% 10% D-Glucose (BD, Franklin Lakes, NJ).

Initiating Cell Culture

A vial of cells stored in media and 5% DMSO was thawed at 37°C and centrifuged at 3,300 x g for 3 minutes. The media/DMSO supernatant was removed and the cells were re-suspended in fresh complete media that had been warmed to 37°C. Cells in media were then transferred into a cell culture flask containing fresh media. Cells were incubated

at 37°C with 5% CO_2. Media was changed every 2-3 days until the cells were ready to be passed.

Passing Cells

Cells were ready for passing when they had reached about 100% confluency in the flask. Old media was aspirated from the cells. Cells were then rinsed with Dulbecco's Phosphate Buffer Saline (DPBS) without Mg^{+2} and Ca^{+2} (Corning Life Sciences). After removing the DPBS, Trypsin EDTA 1X (Corning Life Sciences) was added to the cells and they were incubated at 37°C with 5% CO_2 for 6 minutes. Fresh media was added to the flask, followed by pipetting up and down along the bottom to release any cells remaining on the bottom of the flask and neutralize the trypsin. The cells were centrifuged at 3,300 x g for 3 minutes. The media was aspirated, and the cells were re-suspended in fresh media. Cells (150-300 µL) were then placed in stock flasks for line maintanance or 6-well plates for experimentation.

siRNA Transfection

All siRNAs and transfection reagents were purchased from Santa Cruz Biotechnology (Dallas, TX). The siRNAs are a pool of three siRNA duplexes (Table 2). Each well in 6-well plates were seeded with 300 µL mpkCCD cells in media

and grown to 70%-80% confluency in media lacking in penicillin-streptomycin (24-48 hours). For each transfection, 0.875 µg siRNA (0.438 µg of each siRNA for the TMED2 + TMP21 transfection) were diluted into 100 µL siRNA Transfection Medium (Solution A). Six microliters of siRNA Transfection Reagent were also diluted into 100 µL into transfection medium (Solution B). Solution A was then added to Solution B and incubated for 30 minutes at room temperature.

Media was aspirated from each well and the cells were washed with 2 mL of transfection medium. Eight hundred microliters of transfection medium was added to each of the incubated siRNA transfection reagent mixture (Solution A + Solution B) and immediately overlaid onto the cells. The cells were incubated at 37°C with 5% CO_2 for 7 hours. Fluorescence was observed with an epi-fluorescent microscope before 1 mL of media with 2x FBS and pen-strep was added to each well and incubated at 37°C with 5% CO_2 for 18-20 hours. The transfection solution/2x media was removed and replaced with 4 mL of standard complete media. Cells were ready for experimentation 24-65 hours later.

TABLE 2. siRNA sequences.

siRNA (m)	SEQUENCE
TMED2 A	Sense: CACUAUGACUCCAAAGAUATT Antisense: UAUCUUUGGAGUCAUAGUGTT
TMED2 B	Sense: CCUGUUUAAGAGAGUUAGATT Antisense: UCUAACUCUCUUAAACAGGTT
TMED2 C	Sense: CUGAAUCACCUCUAAUUGATT Antisense: UCAAUUAGAGGUGAUUCAGTT
TMP21 A	Sense: CAAGGCCAUUCUACUAACATT Antisense: UGUUAGUAGAAUGGCCUUGTT
TMP21 B	Sense: CUCCUGUUCUUCAGUGUUATT Antisense: UAACACUGAAGAACAGGAGTT
TMP21 C	Sense: GAAGAGCAUUUGCCUUUGATT Antisense: UCAAAGGCAAAUGCUCUUCTT

Protein Isolation

mpkCCD cells were rinsed with 10 µL DPBS, treated with Gentle Lysis Buffer (GLB) (76.0 mM NaCl, 50 mM Tris-Hcl, 2 mM ethylene glycol tetraacetic acid (EGTA), 1% NP-40, 10% glycerol) and 1 mM phenylmethylsulfonylfluoride (PMSF), and scraped. The cell solution was lysed overnight at 4°C. Cells were centrifuged at 3,300 x g for 5 minutes. The supernatant containing the protein was removed and stored at -20°C or immediately used for experimentation.

BCA ASSAY

Protein concentration was determined using a BCA assay (Thermo Scientific, Rockford, IL). In a 96-well plate, 25 µL bovine serum albumin (2 mg/mL) was placed in a well. A 2-fold dilution was created from the first well over the next 6 wells to create the standards. For the protein sample, 25 µL of a 1:5 dilution was created and placed into the wells. Two hundred microliters of BCA reagent was added to each well that contained the standards and the protein samples. The plate was then incubated at room temperature for 5 minutes before being placed into a 37°C incubator for 15 minutes. Absorbance was measured at 562 nm in a plate reader. A standard curve was created using the absorbances in order to calculate protein concentration.

Western Blotting

Each well of a ExpressPlus PAGE 4-12% Gel (GenScript, Piscataway, NJ) was loaded with 40-100 µg of protein, 1X concentration of NuPAGE LDS Sample Buffer (Invitrogen), and 5% beta-mercaptoethanol that was incubated together at 95°C for 5 minutes. The gel was run at 120 volts for 75 minutes in 1X MOPS Buffer pH 6.8 (GenScript). The gel was then transferred to a nitrocellulose membrane using the Bio-Rad Trans-Blot Turbo Kit (Bio-Rad, Hercules, CA) in the Bio-Rad

Trans-Blot Turbo Transfer System (Bio-Rad) at 1.3 amps/25 volts for 15 minutes. The membrane was incubated in 5 mL of blocking solution (5% w/v non-fat dry milk in Tris-Buffered Saline and 0.1% (v/v) Tween 20 (TBST)) for 30 minutes. A 1:1000 dilution of anti-α ENaC (StressMarq Biosciences, Victoria BC, Canada) was added to the blocking solution and incubated at 4°C with agitation overnight. The following day, the membrane was washed 3 times in 20 mL TBST for 5 minutes each. A goat anti-rabbit HRP conjugated secondary antibody (Jackson ImmunoRearch, West Grove, PA) was then added in a 1:20,000 dilution in 20 mL blocking solution and incubated with agitation for 1 hour. The membrane was then washed 3 times in 20 mL TBST for 5 minutes each. A last wash was performed in 1X Tris-Buffered Saline (TBS) for 10 minutes. A 50% v/v of each of the Western Lightning Plus-ECL Enhanced Chemiluminescence Substrate (PerkinElmer, Waltham, MA) reagents were added and the membrane was imaged using the ChemiDoc XRS+ Stystem (Bio-Rad).

Densitometry Studies

Densitometry studies were performed using ImageJ (http://imagej.nih.gov/ij/). Relative intensities of the bands were then calculated using Microsoft Excel.

CHAPTER III

Results and Discussion

Accessory proteins are critical for the processing, trafficking, and regulating of larger proteins such as ENaC. Distinguishing their roles allows for a deeper understanding of the overall functionality of proteins. In order to identify critical accessory proteins and their necessity in protein processing, a preliminary yeast screen was performed using a yeast deletion library transformed with α-ENaC. Potentially important accessory proteins were then selected for study in a mammalian system naturally expressing the heterotrimeric channel. RNAi was utilized to prevent translation of these accessories.

Silencing accessory proteins in the mammalian cells produces a clearer understanding of the mechanism and pathway a protein undergoes and provides a better picture of regulation. This study examines two possible trafficking proteins, TMED2 and TMP21, which seem to aid in the quantity of ENaC expression.

Sequence Analysis

A sequence analysis was performed for accessory proteins that were found to cause an increase or decrease in ENaC function from a preliminary yeast screen done in the Booth Lab. The protein sequence for each yeast strain was found using the search tool on the *Saccharomyces* Genome Database. The sequence for each strain was then put into BLASTP against a house mouse in order to find the mouse homologs for each strain (Table 3).

Table 3. Mouse homologs of yeast deletion strains.

YEAST STRAIN	YEAST GENE	MOUSE HOMOLOG
YKL073W	LHS1	HYOU1
YMR214W	SCJ1	DNAJA2
YJL073W	JEM1	TID56
YLR372W	SUR4	ELOVL6
YGL054C	ERV14	CNIH4
YGL200C	EMP24	TMED2
YML012W	ERV24	TMED10
YKL126W	YPK1	SGK2
YPL003W	ULA1	NAE1
YPR066W	UBA3	UBA3

Cloning of pESC-Leu/β-ENaC and pESC-Leu/β/γ

Plasmid cloning is a valuable tool that can be utilized to study and analyze expression of proteins in model organisms such as yeast and in mammalian cell culture. Mutation studies and gene knockout studies can be performed on organisms that have been transformed with cloned plasmids. Data from the studies can lead to a better understanding of protein structure and function.

Previous transformations of yeast cells have only been with the α-ENaC subunit. Results could vary when the more efficient heterotrimeric channel is transformed instead. In order to do this, β-ENaC was cloned into pESC-Leu and pESC-Leu/γ. The pESC-Leu plasmid had two MCS sites following galactose promoters, allowing for the insertion of two different genes (FIG 7).

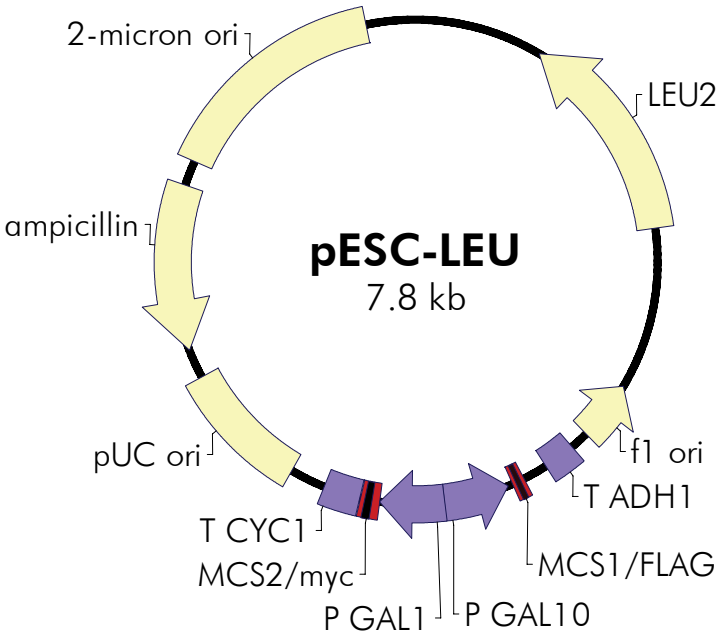

FIG 7. pESC-Leu plasmid map. γ-ENaC was cloned into the MCS1 site under a GAL10 promoter. β-ENaC was cloned into the MCS2 site under a GAL1 promotor.

The β-ENaC gene, which is about 2 kb, on the plasmid pCMV-Myc/β-ENaC was amplified through PCR. Amplification of the β-ENaC gene was confirmed via a 0.8% w/v agarose gel (FIG 8, lanes 2 and 3). The PCR product was digested along with pESC-Leu plasmid using XhoI and NheI restriction enzymes. The digestion products were analyzed by gel electrophoresis using a 0.8% w/v agarose gel (FIG 9). The pESC-Leu plasmids are 7.8 kb but once linearized, the fragment seemed to run larger at about 10 kb (FIG 9A, lane 2). The β-ENaC fragments were where it is expected to be at 2 kb.

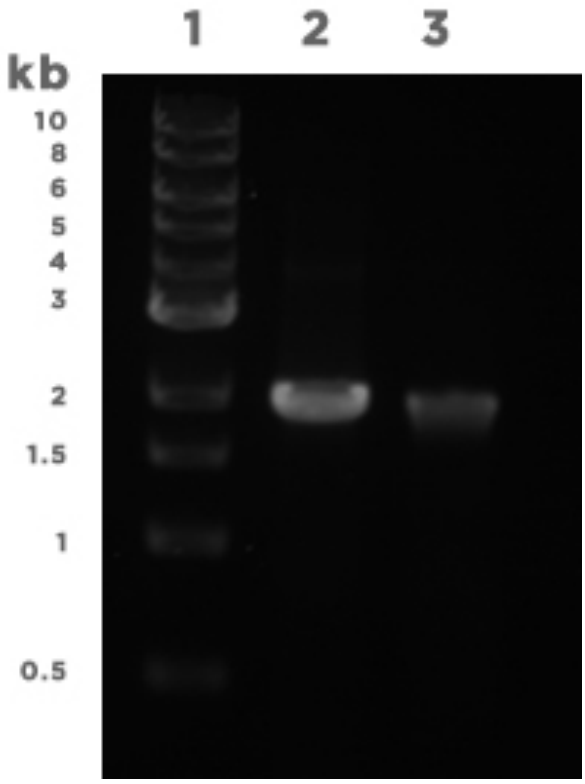

FIG 8. β-ENaC PCR product. *lane 1*, 1 kb ladder. *lanes 2-3,* PCR product of β-ENaC at 2 kb.

The digested pESC-Leu plasmid fragments (FIG 9A, lane 2) and β-ENaC (FIG 9A, lane 3) were gel extracted, cleaned, and quantitated. The fragments were then ligated for 30 minutes at room temperature with NEB T4 DNA Ligase. The reactions were transformed into NEB 5-alpha *E. coli* cells and grown on LB+AMP agar plates overnight at 37°C. Colonies from the transformation were grown overnight in liquid cultures of LB+AMP, and pESC-Leu/β-ENaC was isolated using QIAprep Spin Miniprep Kit.

Confirmation of the cloned plasmids was verified via agarose gel electrophoresis (FIG 9B). pESC-Leu/β-ENaC was digested with XhoI and NheI in order to verify cloning. Fragments at 7.8 kb and 2 kb indicate that the β-ENaC gene had been removed (FIG 9B, lane 4). pESC-Leu/β-ENaC was also digested with AgeI and NcoI. Expected fragments using NEBcutter V2.0 were 5.1 kb, 2.1 kb, doublets at 0.750 and 0.709 kb, 0.516 kb, and 0.366 kb. Fragments on the gel (FIG 9B, lane 5) matched those that were predicted by NEBcutter except for the 2.1 kb fragment. AgeI is most efficient at 25°C. Having ran the digestion at 37°C could have caused the cutting of the 2.1 kb fragment into the two smaller fragments seen in the gel. Clones of the pESC-Leu/β-ENaC plasmid were sequenced at Quintara Biosciences and compared to theoretical sequences using ClustalW2.

The entire β-ENaC cloning strategy was then used to clone β-ENaC into pESC-Leu/γ-ENaC that had previously been created in the Booth Lab (FIG 10). pESC-Leu/γ-ENaC (FIG 10A, lane 5), which is 11.8 kb, was gel extracted along with β-ENaC at 2 kb (FIG 10A, lane 6). FIG 10B was the conformation gel showing the cloned plasmids. pESC-Leu/β/γ was digest with XhoI and NheI in order to verify insertion of the β-ENaC gene into pESC-Leu/γ-ENaC. DNA fragments at 11.8 kb and 2 kb (FIG 10B, lane 5), indicated cloning of

the gene into the plasmid. pESC-Leu/β/γ was also double digested with AgeI and NcoI. The results of the digestion matched the predicted results from NEBcutter, which were 5.1 kb, 2.7 kb, 1.4 kb, doublets at 0.750 and 0.709 kb, 0.516 kb, and 0.366 kb.

An agarose gel was run with pESC-Leu and both of the cloned plasmids in order to verify cloning (FIG 11). pESC-Leu is 7.8 kb. With the addition of β-ENaC, the cloned plasmid would be 9.8 kb. γ-ENaC is also 2 kb. A plasmid with both of the β- and γ-ENaC would run on an agarose gel at 11.8 kb. That is what is seen in Figure 11. Extra fragments seen in lanes 2-4 are supercoiled forms of the plasmids.

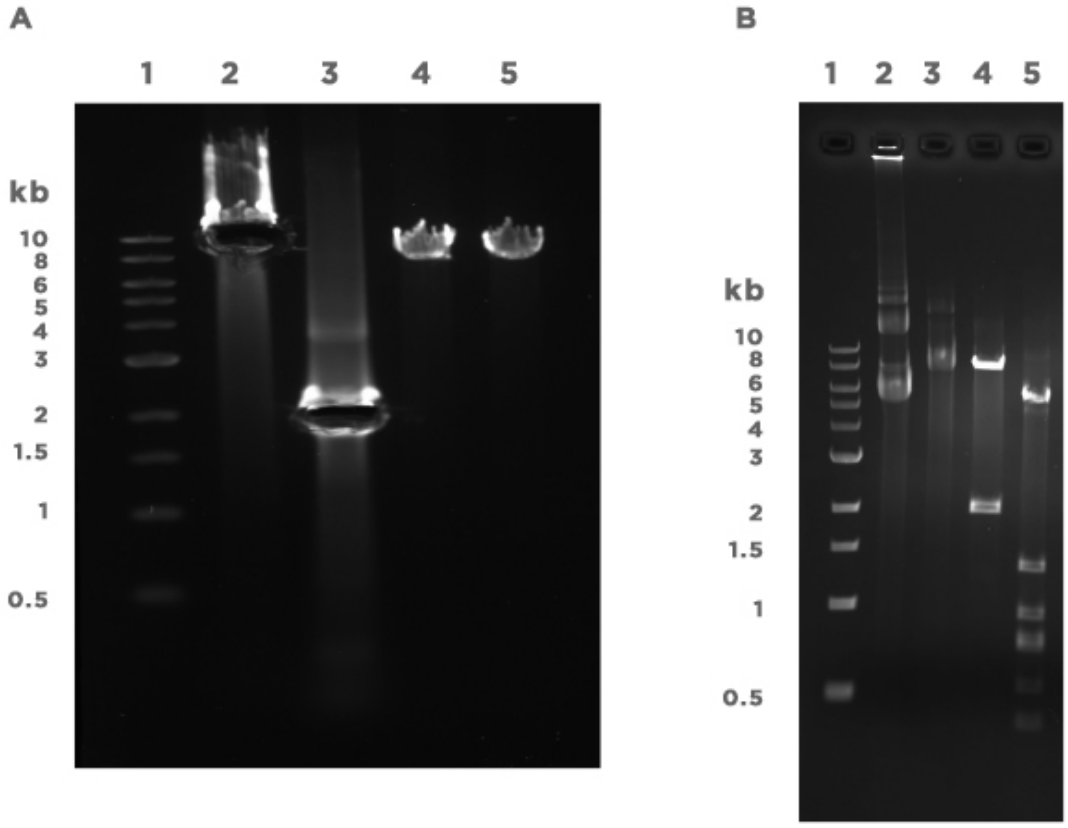

FIG 9. pESC-Leu/β-ENaC cloning and confirmation. (A) Digested pESC-Leu and β-ENaC were separated on a 0.8% w/v agarose gel before being gel extracted and ligated. *lane 1*, 1 kb ladder. *lane 2*, pESC-Leu digested with XhoI and NheI. *lane 3*, β-ENaC digested with XhoI and NheI. *lane 4*, pESC-Leu single digestion control with XhoI. *lane 5*, pESC-Leu single digestion control with NheI. **(B)** Confirmation gel of the cloned pESC-Leu/β-ENaC. *lane 1*, 1 kb ladder. *lane 2*, pESC-Leu control. *lane 3*, pESC-Leu/β-ENaC control. *lane 4*, pESC-Leu/β-ENaC digested with XhoI and NheI. *lane 5*, pESC-Leu/β-ENaC digested with AgeI and NcoI.

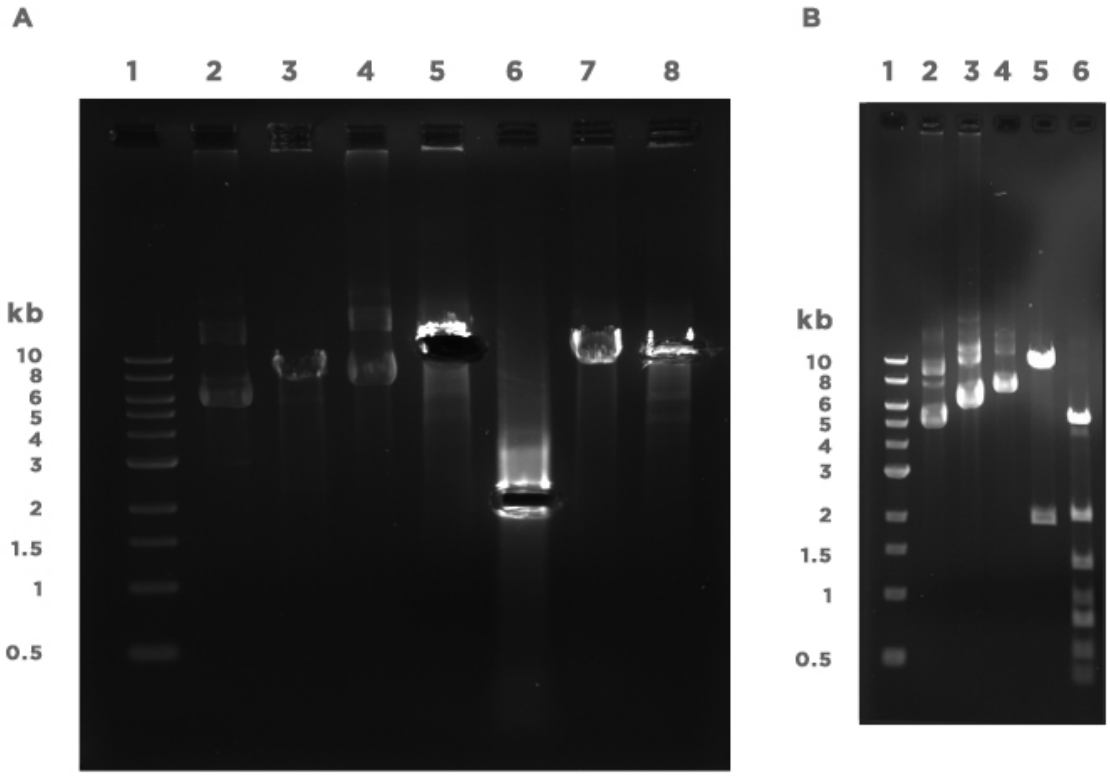

FIGURE 10. pESC-Leu/β/γ cloning and confirmation. (A) Digested pESC-Leu/γ-ENaC and β-ENaC were separated on a 0.8% w/v agarose gel before being gel extracted and ligated. *lane 1*, 1 kb ladder. *lane 2*, pESC-Leu control. *lane 3*, pESC-Leu control digested with XhoI and NheI. *lane 4*, pESC-Leu/γ-ENaC control. *lane 5*, pESC-Leu/γ-ENaC digested with XhoI and NheI. *lane 6*, β-ENaC digestion with XhoI and NheI. *lane 7*, pESC-Leu/γ-ENaC single digestion control with XhoI. *lane 8*, pESC-Leu/γ-ENaC single digestion control with NheI. **(B)** Confirmation gel of the cloned pESC-Leu/β-ENaC. *lane 1*, 1 kb ladder. *lane 2*, pESC-Leu control. *lane 3*, pESC-Leu/γ-ENaC control. *lane 4*, pESC-Leu/β/γ control. *lane 5*, pESC-Leu/β/γ digested with XhoI and NheI. *lane 6*, pESC-Leu/β/γ digested with AgeI and NcoI.

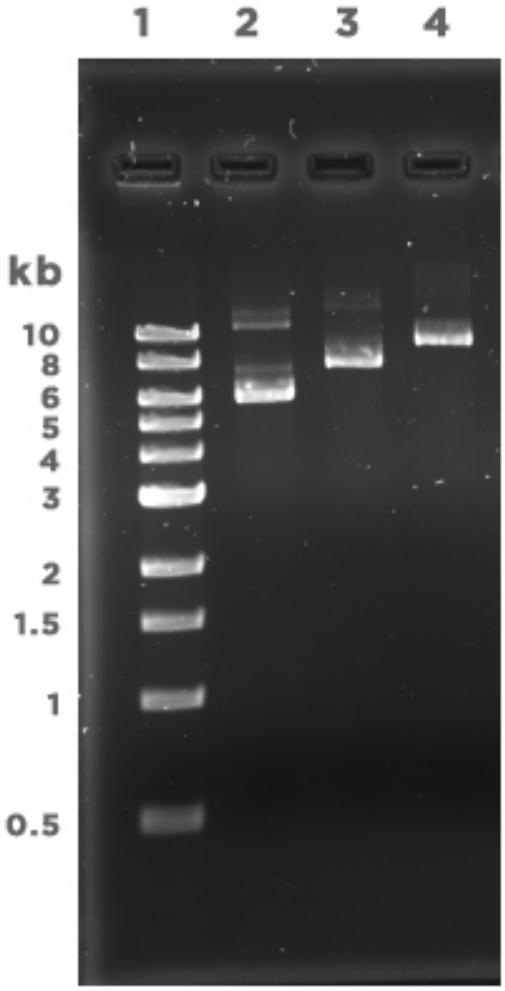

Figure 11. Agarose gel with cloned plasmids. Gel electrophoresis of the cloned plasmids against the original pESC-Leu (about 7.8 kb) indicates the genes were cloned into the plasmid. Both β- and γ-ENaC are about 2 kb, making the pESC-Leu/γ-ENaC 9.8 kb and the pESC-Leu/β/γ 11.8 kb. *lane 1*, 1 kb ladder. *lane 2*, pESC-Leu. *lane 3*, pESC-Leu/β-ENaC. *lane 4*, pESC-Leu/β/γ.

Antibody Screen

An antibody screen was performed in order to find an efficient antibody against individual ENaC subunits in mpkCCD cells. Normal α-ENaC has a molecular weight of about

76,000 Daltons, while both β- and γ-ENaC have molecular weights of about 70,000 Daltons. All three subunits are glycosylated and cleaved as part of processing in order to produce fully functioning ENaC within the cell surface.

mpkCCD cells were grown to confluency in complete media. Cells were then rinsed with DPBS, treated with GLB+PMSF, scraped, and incubated overnight at 4°C in order to isolate total protein. The cellular debris was pelleted and discarded and protein concentration in the supernatant was determined using the BCA Assay.

A western blot was performed on protein extracted from the mpkCCD cells. A 4-12% SDS-PAGE acrylamide gel was loaded with 100 µg of protein then transferred to a nitrocellulose membrane. The membranes were probed with anti- α, β, or γ ENaC primary antibody from StressMarq, as well as an anti-α ENaC primary antibody from Millipore (FIG 12).

The antibodies from StressMarq each had cross reactivity with ENaC from mpkCCD cells. The anti-α ENaC antibody bound the glycosylated form of the α-ENaC between 90,000 and 110,000 Daltons (Figure 12A). There seems to also be a high amount of non-specific binding. This can be due to the fact that all of the subunits share a 30-40% homology, and this antibody can be cross reacting with the

other subunits as well as any glycosylated and cleaved products from all of the subunits. The anti-β and γ ENaC antibody bound to both the glycosylated and cleaved forms of the subunit (Figure 12B and 12C).

The anti-α ENaC antibody from Millipore had cross reactivity with the α-ENaC subunit. Figure 12D indicates the antibody cross-reacted with the normal and cleaved forms of α-ENaC.

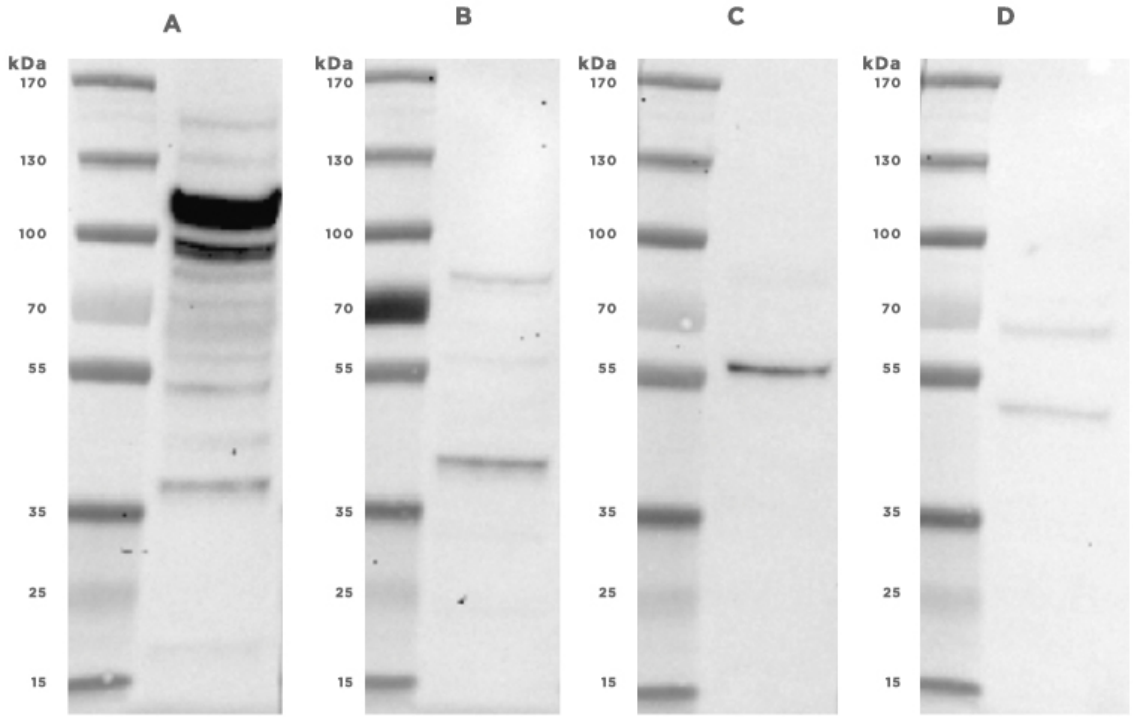

FIG 12. Primary antibody screen against α-, β-, and γ-ENaC. **(A)** Anti- α ENaC primary antibody from StressMarq reacted with glycosylated forms of α-ENaC. **(B)** Anti- β ENaC primary antibody from StressMarq bound to both the normal and cleaved forms of β-ENaC. **(C)** Anti- γ ENaC primary antibody from StressMarq bound to both the normal and cleaved forms of γ-ENaC. **(D)** Anti- α ENaC primary antibody from Millipore reacted with both the normal and cleaved forms of α-ENaC.

ENaC expression levels during TMED2 and TMP21 silencing

A mammalian cell culture lab using murine principal kidney cortical collecting duct cells (mpkCCD) that were initiated from frozen stocks under sterile conditions was created. The cells were thawed at 37°C and centrifuged briefly. The supernatant was removed and the cells were resuspended in serum free media containing fetal bovine serum, insulin, and penicillin. Cells were grown in culture flasks with standard growth media at 37°C with 5% CO_2 until confluent.

siRNA experiments were performed in 6-well plates when the mpkCCD cells reached about 80% confluency. Once confluent, the mpkCCD cells were transfected with the siRNAs for the accessory proteins TMED2 and TMP21 alone and in combination. Controls included a siRNA negative control with a scrambled sequence, a fluorescein isothiocyanante (FITC) control with a scrambled siRNA sequence, cells incubated with the transfection reagents only in order to monitor for toxicity, and a well with untreated cells grown in standard media. The siRNAs and transfection reagents were diluted in transfection medium and incubated for 30 minutes at room temperature. The cells were rinsed with transfection medium and incubated with the siRNA solution at 37°C with 5% CO_2 for 7 hours. After 7 hours, the

fluorescent control was observed with an epi-fluorescent microscope. The FITC conjugated siRNA control could be seen in various locations throughout the cells (FIG 13). The scrambled sequence would prevent the siRNAs from knocking down the genes in the control cells but does not interfere in any other cellular messaging. As a control, fluorescence within the cells indicated the siRNAs had entered the cell.

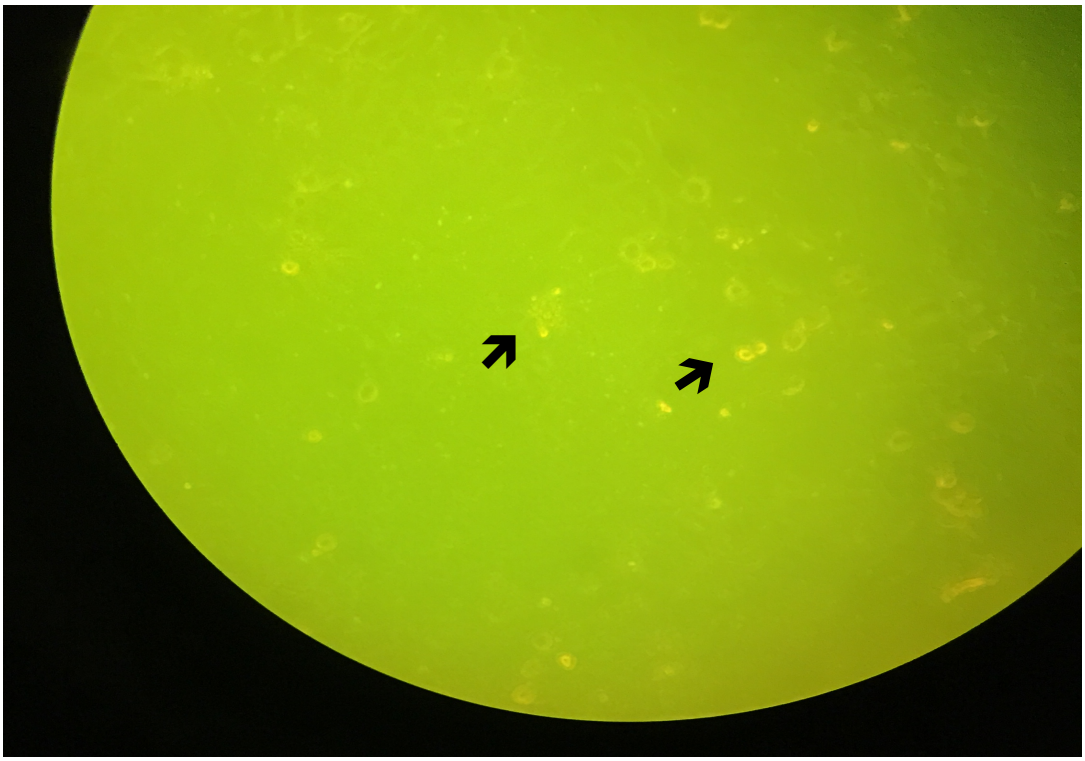

FIG 13. Transfected fluorescent siRNAs in mpkCCD cells. FITC conjugated siRNAs with a scrambled sequence were transfected into mpkCCD cells as a control. Fluorescence within the cells indicated the siRNAs had entered into the cell.

Media containing twice the amount of FBS and pen/strep was added to cells that had been transfected in order to aid in cell recovery. Cells were incubated at 37°C with 5% CO_2 for 20 hours to complete the transfection. After 24 hours, the transfected cells were ready to be harvested for total protein. Cells were rinsed with DPBS, scraped in GLB+PMSF, and incubated overnight at 4°C in order to isolate total protein lysate.

The cellular debris was pelleted and discarded and protein concentration in the supernatant was determined using the BCA Assay. Protein concentrations ranged from 0.7 µg- 1.7 µg. Equal amounts of each protein sample (between 40-100 µg) were separated in a 4-12% SDS-PAGE acrylamide gel and transferred to a nitrocellulose membrane. The membrane was probed with an anti-βENaC primary antibody in blocking solution overnight at 4°C with agitation. The membrane was rinsed and then probed with a HRP secondary antibody in blocking solution for 1 hour then rinsed. A chemiluminescent substrate was added to the membrane and it was imaged (FIG 14A). The western blot membranes were then stripped and re-probed with an anti-β actin primary antibody to determine the consistency of loading (FIG 14B). Results indicated that protein was loaded at a consistent concentration and the results seen in Figure 14A are not

due to loading differences.

In Figure 14A, strong β-ENaC bands were observed at approximately 60 kDa in the control lanes (lanes 5-7). Based on densitometry studies using ImageJ, the intensities of the β-ENaC bands were decreased by 48.96% and 52.91% (FIG 14A, lane 2), respectively, when TMED2 siRNas were transfected into the cells and compared to the untreated cells (FIG 14A, lane 7). TMP21 siRNA transfections (FIG 14A, lane 3) caused a decrease by 71.12% and 54.48% when compared to the untreated cells (FIG 14A, lane 7).

Cells co-transfected with both siRNAs displayed a decrease in expression by 89.10% and 65.67% (FIG 14A, lane 4), respectively, compared to the untreated control cells (FIG 14A, lane 7). A greater decrease was expected with the double knockdowns since more proteins should have been silenced. The densitometry studies indicated that decrease in expression was about the same as the single knockdowns. This may be due to the design of the siRNAs from Santa Cruz Biotechnology. Since each siRNA contains a pool of three sequences, introduction of six different sequences may be hindering and overwhelming the siRNA machinery. This would prevent efficient knockdown of either protein and could be a possible reason as to why the double knockdowns did not show an increased reduction of ENaC expression.

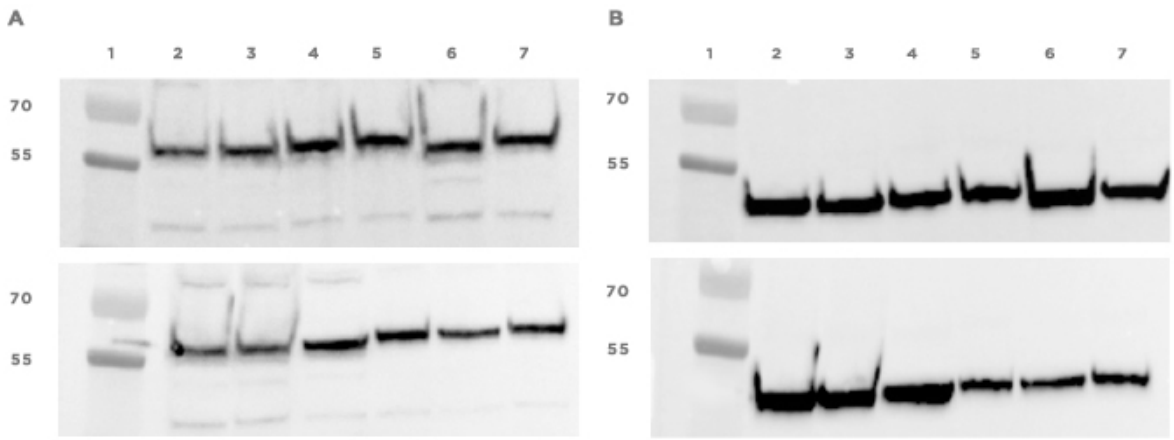

FIG 14. Western blots of siRNA-treated mpkCCD cells. (A) Western blots from two independent trials indicated the cells treated with the siRNAs TMED2 and TMP21 expressed a lower quantity of ENaC than the controls by the intensity of the corresponding bands. Blots were probed with anti- β ENaC from StressMarq. *lane 1,* kDa Ladder. *lane 2,* TMED2. *lane 3,* TMP21. *lane 4,* TMED2+TMP21. *lane 5,* siRNA negative control. *lane 6,* reagent only control. *lane 7,* untreated cells. **(B)** The western blots from (A) were stripped and reprobed with anti-β actin primary antibody as a loading control. *lane 1,* kDa Ladder. *lane 2,* TMED2. *lane 3,* TMP21. *lane 4,* TMED2+TMP21. *lane 5,* siRNA negative control. *lane 6,* reagent only control. *lane 7,* untreated cells.

A decrease in expression in the cell can be due to the disruption of trafficking of ENaC subunits to the Golgi. Since TMED/p24 proteins are involved in the vesicular transport of immature proteins to the Golgi for further processing, knockdown of these proteins can prevent ENaC from fully undergoing posttranslational modification and localizing to the cell membrane. Specifically, TMED proteins seem to be required to transport GPI-anchored proteins to the membrane[22]. Any disruption of transport of

these signaling proteins could be affecting ENaC, which could also explain a decrease in expression.

Studies have indicated that knockdown of TMED2 destabilizes protein complexes that also contain TMP21[22]. By silencing these genes, complexes that were used to transport, process, and regulate ENaC could be disrupted. It is also possible for the ENaC subunits to be misfolding if either TMED2 or TMP21 are involved as chaperone proteins[22].

Trafficking storage pools of ENaC may also have been affected by the silencing of TMED2 and TMP21. ENaC is often recycled and stored in vesicles in the intracellular space after having been removed from the apical membrane[17]. This allows for rapid mobilization from cAMP and aldosterone stimuli in times of low blood pressure. By knocking down TMED proteins, it may have interfered with the volume of ENaC being able to be stored in the vesicles.

Functional Studies

In an effort to monitor changes in the ENaC function, sodium transport across epithelia, mpkCCD cells were also seeded on Transwell® Permeable Support membrane plates. These plates contain a permeable polycarbonate membrane that allows polarized cells, such as mpkCCD cells, to

intake and secrete metabolic molecules on both the apical and basolateral membranes. This creates an environment that allows the cells to carry out metabolic activities in a way that is similar to what is found *in vivo*.

The cells were transfected with siRNA when at 80% confluency. mpkCCD cells were grown for 24-48 hours until a monolayer formed and then transfected with siRNA and controls described above in the expression study. Voltage was measured 24, 48, and 72 hours after transfection. No voltage changes were detected in either the transfected cells or untreated control cells (data not shown). This may be due to the mpkCCD cells not forming a tight monolayer across the permeable membrane. A failure to form a tight junction of cells would prevent the cells from controlling the amount of sodium that is passing through the cells and permeable membrane, thus preventing a voltage change. Repeated trials yielded the same results.

CHAPTER IV

Conclusions

Many ion channels are difficult to isolate and purify, making it complicated to fully understand their functionality and mechanism. ENaC is no exception. As a result, other biochemical studies are needed in order to gather information for further understanding of these channels. In the current study, RNAi has proven to be a beneficial tool as a means to study trafficking, assembly, and regulation of ENaC.

Studying accessory proteins is vital in understanding the processing and trafficking of ENaC. This study has shown the essential role of TMED/p24 proteins are to the expression of ENaC. Cells with a knockdown of just one of the proteins exhibited a decreased expression level in western blots compared to those cells treated with scrambled sequences and untreated cells. These results confirm a positive direction for further studying accessory proteins using RNAi. They provide a successful method and lay the groundwork for identifying additional proteins that are critical to the full functionality of ENaC in future studies.

REFERENCES

(1) Go, A. S., Mozaffarian, D., Roger, V. L., Benjamin, E. J., Berry, J. D., Borden, W. B., Bravata, D. M., Dai, S., Ford, E. S., Fox, C. S., Franco, S., Fullerton, H. J., Gillespie, C., Hailpern, S. M., Heit, J. A., Howard, V. J., Huffman, M. D., Kissela, B. M., Kittner, S. J., Lackland, D. T., Lichtman, J. H., Lisabeth, L. D., Magid, D., Marcus, G. M., Marelli, A., Matchar, D. B., McGuire, D. K., Mohler, E. R., Moy, C. S., Mussolino, M. E., Nichol, G., Paynter, N. P., Schreiner, P. J., Sorlie, P. D., Stein, J., Turan, T. N., Virani, S. S., Wong, N. D., Woo, D., and Turner, M. B. (2013) Heart Disease and Stroke Statistics—2013 Update A Report From the American Heart Association. *Circulation 127*, e6–e245.

(2) http://www.cdc.gov/features/dssodium/.

(3) Rossier, B. C., Staub, O., and Hummler, E. (2013) Genetic dissection of sodium and potassium transport along the aldosterone-sensitive distal nephron: Importance in the control of blood pressure and hypertension. *FEBS Lett. 587*, 1929–1941.

(4) CDC. (2012) Vital signs: awareness and treatment of uncontrolled hypertension among adults—United States, 2003–2010. *MMWR 61*, 703–709.

(5) Green, W. N., and Millar, N. S. (1995) Ion-channel assembly. *Trends Neurosci. 18*, 280–287.

(6) Garty, H., and Palmer, L. G. (1997) Epithelial sodium channels: function, structure, and regulation. *Physiol. Rev.* 77, 359–396.

(7) Kashlan, O. B., and Kleyman, T. R. (2011) ENaC structure and function in the wake of a resolved structure of a family member. *Am. J. Physiol. - Ren. Physiol. 301*, F684–F696.

(8) Staruschenko, A. (2011) Regulation of Transport in the Connecting Tubule and Cortical Collecting Duct, in *Comprehensive Physiology*. John Wiley & Sons, Inc.

(9) Snyder, P. (2002) The Epithelial Na+ Channel: Cell Surface Insertion and Retrieval in Na+ Homeostasis and Hypertension. *Endocr. Rev. 23*, 258–275.

(10) Kellenberger, S., and Schild, L. (2002) Epithelial Sodium Channel/Degenerin Family of Ion Channels: A Variety of Functions for a Shared Structure. *Physiol. Rev. 82*, 735–767.

(11) Stewart, A. P., Haerteis, S., Diakov, A., Korbmacher, C., and Edwardson, J. M. (2011) Atomic Force Microscopy Reveals the Architecture of the Epithelial Sodium Channel (ENaC). *J. Biol. Chem. 286*, 31944–31952.

(12) Canessa, C. M., Schild, L., Buell, G., Thorens, B., Gautschi, I., Horisberger, J.-D., and Rossier, B. C. (1994) Amiloride-sensitive epithelial Na+ channel is made of three homologous subunits. *Nature 367*, 463–467.

(13) De la Rosa, D. A., Canessa, C. M., Fyfe, G. K., and Zhang, P. (2000) Structure and Regulation of Amiloride-Sensitive Sodium Channels. *Annu. Rev. Physiol. 62*, 573–594.

(14) Stockand, J. D., Staruschenko, A., Pochynyuk, O., Booth, R. E., and Silverthorn, D. U. (2008) Insight toward epithelial Na+ channel mechanism revealed by the acid-sensing ion channel 1 structure. *IUBMB Life 60*, 620–628.

(15) Wiemuth, D., Lott, J. S., Ly, K., Ke, Y., Teesdale-Spittle, P., Snyder, P. M., and McDonald, F. J. (2010) Interaction of Serum- and Glucocorticoid Regulated Kinase 1 (SGK1) with the WW-Domains of Nedd4-2 Is Required for Epithelial Sodium Channel Regulation. *PLoS ONE 5*, e12163.

(16) Rossier, B. C. (2014) Epithelial sodium channel (ENaC) and the control of blood pressure. *Curr. Opin. Pharmacol. 15*, 33–46.

(17) Edinger, R. S., Bertrand, C. A., Rondandino, C., Apodaca, G. A., Johnson, J. P., and Butterworth, M. B. (2012) The Epithelial Sodium Channel (ENaC) Establishes a Trafficking Vesicle Pool Responsible for Its Regulation. *PLoS ONE 7*, e46593.

(18) Asher, C., Sinha, I., and Garty, H. (2003) Characterization of the interactions between Nedd4-2, ENaC, and sgk-1 using surface plasmon resonance. *Biochim. Biophys. Acta BBA - Biomembr. 1612*, 59–64.

(19) Gumz, M. L., Stow, L. R., Lynch, I. J., Greenlee, M. M., Rudin, A., Cain, B. D., Weaver, D. R., and Wingo, C. S. (2009) The circadian clock protein Period 1 regulates expression of the renal epithelial sodium channel in mice. *J. Clin. Invest. 119*, 2423–2434.

(20) De la Rosa, D. A., Navarro-Gonzalez, J. F., and Giraldez, T. (2013) ENaC Modulators abd Renal Disease. *Curr. Mol. Pharmacol. 6*, 35–43.

(21) Bens, M., Vallet, V., Cluzeaud, F., Pascual-Letallec, L., Kahn, A., Rafestin-Oblin, M. E., Rossier, B. C., and Vandewalle, A. (1999) Corticosteroid-Dependent Sodium Transport in a Novel Immortalized Mouse Collecting Duct Principal Cell Line. *J. Am. Soc. Nephrol. 10*, 923–934.

(22) Jerome-Majewska, L. A., Achkar, T., Luo, L., Lupu, F., and Lacy, E. (2010) The trafficking protein Tmed2/p24β1 is required for morphogenesis of the mouse embryo and placenta. *Dev. Biol. 341*, 154–166.